Journal of Advanced Pharmacy Research

Section D: Drug Design, Delivery and Targeting

A Molecular Docking Study Conducted on the Model of Tyrosinase-Related Protein 1 from [PDB ID: 5M8T] Using Kojic Acid and Its Structural Analogs as Inhibitors

Roohallah Yousefi[1, 2, *]

[1]*Research Affairs, Behbahan Faculty of Medical Sciences, Behbahan, Iran.*
[2]*Department of Biochemistry, Faculty of Biological Sciences, Tarbiat Modares University, Tehran, Iran.*

Corresponding author: Roohallah Yousefi, Research Affairs, Behbahan Faculty of Medical Sciences, Behbahan, Iran. Tel.: +989168741235
E-mail address: r.yosofei@modares.ac.ir

To cite this article: Yousefi, R. A Molecular Docking Study was Conducted on the Model of Tyrosinase-related Protein 1 from [PDB ID: 5M8T] Using Kojic Acid and its Structural Analogs as Inhibitors. *J. Adv. Pharm. Res.* **2025**, *9* (1), 41-61. DOI: 10.21608/aprh.2024.310212.1286

ABSTRACT

Background: Kojic acid and its related compounds, such as β-arbutin, α-arbutin, and deoxyarbutin, are known for inhibiting tyrosinase activity, which is crucial for melanin production in the skin. Kojic acid acts as a chelating agent that binds to copper ions in tyrosinase, inhibiting its activity. β-arbutin and α-arbutin are natural compounds that competitively inhibit tyrosinase by releasing hydroquinone upon absorption into the skin. Deoxyarbutin, a synthetic derivative, is a potent inhibitor of tyrosinase due to its stability and ability to bind to copper ions, preventing the oxidation of tyrosine and DOPA. These compounds effectively reduce melanin production, resulting in a lighter complexion by interfering with the melanin synthesis pathway through tyrosinase inhibition. **Objectives:** In the present study, we investigate the affinity of binding and binding site of kojic acid and its analogues for the inhibition of tyrosinase-related protein 1. **Methods:** In this study, we utilized the tyrosinase-related protein 1 (TYRP1) model from the Protein Data Bank (PDB) with the [PDB ID: 5M8T]. Molecular docking was performed using the Molegro Virtual Docker tool with models of 22 ligand compounds from the PubChem database, including kojic acid and its analogues. The physicochemical properties and pharmacokinetics of the compounds were predicted using the SwissADME web tool. **Results:** Our study identified various binding sites of kojic acid and its analogues on TRP1, which included amino acids such as Gln78, Gly209, Glu210, Val211, Asp212, Phe213, His215, Glu216, Tyr348, Ser349, Pro431, Ile432, and His434. These compounds showed high gastrointestinal absorption, inability to cross the blood-brain barrier, no inhibition of cytochrome P450 enzymes, and not being Pgp substrates. Additionally, they exhibited minimal skin absorption. **Discussion:** Our study examined 22 analog compounds of kojic acid, which exhibited high gastrointestinal absorption but lacked permeability through the blood-brain barrier. All of the studied compounds, consisting of Kojic acid and β-arbutin, exhibit effective binding affinity and binding sites for the inhibition of TYRP1. **Conclusion:** This study provides evidence supporting the effectiveness of kojic acid and its similar compounds in inhibiting TYRP1 activity, which could be valuable in the treatment of skin conditions related to hyperpigmentation.

Keywords: Kojic acid, Hyperpigmentation, TYRP1.

INTRODUCTION

Dark skin and age spots are common cosmetic concerns that can affect individuals of all ages. While there are various treatments available, some natural remedies have shown promise in reducing the appearance of dark skin and age spots. This article will review the evidence for several natural remedies and discuss their potential benefits and limitations [1, 2]. Turmeric, a spice commonly used in Indian and Middle Eastern cuisine, has been shown to have anti-inflammatory and antioxidant properties that can help lighten the skin [3]. Turmeric extract has been found to reduce melanin production in human skin cells [3]. Additionally, Vitamin C-rich foods, such as citrus fruits and leafy greens, have also been shown to have antioxidant properties that can help protect the skin from damage caused by free radicals [1, 4].

Other natural remedies that have been found to be effective in reducing dark skin and age spots include pomegranate extracts, which have antioxidant and anti-inflammatory properties [1, 5].

In addition to these natural remedies, maintaining good hygiene practices such as regularly cleansing the skin and using sunscreen can also help prevent darkening of the skin [4]. Camouflage therapy, which involves using makeup or clothing to conceal the affected area, can also be effective in reducing the appearance of age spots [6].

Melanin synthesis is a complex process that involves the conversion of L-phenylalanine to L-tyrosine, followed by the hydroxylation of L-tyrosine to 3,4-L-dihydroxyphenylalanine (L-DOPA) [7]. This process is catalyzed by the enzyme tyrosinase, which is present in the melanocytes of the skin [8]. The melanocortin system plays a crucial role in regulating melanin synthesis by controlling the expression of tyrosinase and other melanogenic enzymes. The melanocortin peptides α-, β-, and γ-melanocyte-stimulating hormone (MSH) and adrenocorticotropic hormone (ACTH) are produced by the pituitary gland and stimulate melanin synthesis by binding to their respective receptors on the surface of melanocytes [9].

In addition to the melanocortin system, other signaling pathways also play a role in regulating melanin synthesis. For example, the KIT signaling pathway upregulates the expression of MITF, a transcription factor that plays a key role in melanogenesis. The Wnt signaling pathway also regulates melanin synthesis by controlling the expression of β-catenin, a protein that is involved in the development of melanocytes [10].

Excessive melanin synthesis can lead to hyperpigmentation, which can have negative effects on skin appearance and increase the risk of malignant melanoma [7]. Therefore, inhibiting tyrosinase activity is an effective way to prevent excessive melanin synthesis.

Kojic acid and β-arbutin are two well-known depigmenting agents that have been shown to inhibit tyrosinase activity [11, 12]. These compounds are commonly used as positive controls in assays to screen for emerging components or extracts that effectively inhibit melanin synthesis. α-Arbutin is a synthetic counterpart of β-arbutin and has been shown to inhibit melanogenesis in human skin cells [11, 12]. Deoxyarbutin is a derivative of β-arbutin that has been shown to be more potent than its parent compound as an inhibitor of tyrosinase activity [13]. Melanin synthesis is a complex process that involves multiple signaling pathways and enzymes. Inhibiting tyrosinase activity is an effective way to prevent excessive melanin synthesis and associated negative effects on skin appearance and health. In the present study, we investigate the affinity of binding and binding site of kojic acid and its analogues for the inhibition of tyrosinase-related protein 1.

MATERIAL AND METHODS

Preparation of the Model [PDB ID: 5M8T]

The molecular model of the 3D structure of human tyrosinase-related protein 1 (TRP1) in complex with tropolone [PDB ID: 5M8T] was obtained from the RCSB PDB database. The 5M8T structure was crystallized using X-ray diffraction. The protein was expressed in an insect type, Spodoptera frugiperda, and contains specific mutations (T391V, R374S, and Y362F). The structure was determined at a resolution of 2.35 Å, indicating a high level of precision. The R-Values indicate that the structure refinement was good, with R-Values Free, Work, and Observed at 0.225, 0.183, and 0.185, respectively. This information can be useful for understanding the function and interactions of TRP1 with other molecules [2].

Ligand Model Preparation

To prepare ligand molecular models for further analysis, 22 compounds consisting of kojic acid and its analogues were collected from the PubChem database (14) (**Table 1**). The Molegro Virtual Docker tool was used for this purpose [15].

The SwissADME Web Tools

The SwissADME web tool is a valuable resource for predicting physicochemical properties and pharmacokinetics of compounds during the early stages of drug discovery and development. It utilizes various predictive models to assess Lipinski's Rule of Five, a set of guidelines that determine a molecule's likelihood of being orally active. These guidelines consider molecular weight, logP, hydrogen bond donors, hydrogen bond acceptors, and rotatable bonds. SwissADME predicts passive gastrointestinal absorption and brain penetration using the BOILED-Egg model. It also predicts other properties such as solubility, drug-likeness, and

pharmacokinetic profiles. These predictions are crucial for understanding bioavailability and safety [16-20].

Molecular Docking Study

Molecular docking is a computational technique that predicts the binding orientation of small molecules to macromolecular targets. Molegro Virtual Docker (MVD) is a powerful tool that accounts for both rigid and flexible interactions. By generating accurate predictions of binding affinities and interaction patterns, MVD considers the dynamic nature of biological systems where ligands and receptors adopt multiple conformations. Its grid-based scoring functions evaluate the interaction energy between the ligand and receptor at discrete points in space, allowing for the efficient evaluation of many possible ligand conformations (15).

RESULTS

In our study, we investigated tyrosinase inhibitor ligands such as kojic acid and its analogues. The compound with CID Number 153883063 exhibited the highest affinity for the binding site on the molecular model of tyrosinase-related protein 1, with the highest ligand efficiency (LE1) of -10.487 (kcal/mol). The strongest hydrogen bond of -12.8858 (kcal/mol) was formed by the combination of CID Number 88097838 with tyrosinase-related protein 1 (**Table 2**).

Compounds with CID Numbers 79869776, 79021271, 10511097, 234556, 164954, and 3840 are linked to a binding site containing amino acids Gln78, Gly209, Glu210, Val211, Asp212, Phe213, His215, Glu216, Tyr348, Ser349, Pro431, Ile432, and His434 from the sequence of tyrosinase-related protein 1.
Compounds with CID Numbers 97371, 98896, 2747691, 6451652, 18407654, 18922783, 88588069, and 153883063 are associated with the binding site containing amino acids His192, His215, His377, Asn378, His381, Leu382, Gly389, Gln390, Val391, and Ser394, Phe400 from the tyrosinase-related protein 1 sequence.

Compounds with CID Numbers 20579588, 79872385, and 118244682 bind to a binding site containing amino acids Cys113, Arg114, Pro115, Gly116, Thr226, Leu229, Arg230, Glu232, Lys233, and Gln236 of the tyrosinase-related protein 1 sequence.
Compounds with CID Numbers 9869622, 18678805, 25202640, and 88097838 are attached to a binding site containing amino acids Arg84, Asp85, Asp86, Arg87, Arg165, Ser166, Tyr194, Lys197, Lys198, Thr199, and Phe200, Leu302 from the sequence of tyrosinase-related protein 1.

The compound with CID Number 138581133 is linked to the binding site including amino acids Val68, Thr69, Thr98, Cys99, His100, Cys101, Asn439, Pro445, and Pro446 (**Figure 1, 2,** and **3**).

Physicochemical Properties of Studied Compounds:

The weights of the compounds studied ranges from 143.117 to 269.013 daltons, with a number of heavy atoms between 10 and 16. Most compounds have 1 to 3 rotatable bonds, indicating low flexibility. The majority of hydrogen bond acceptor groups have 4 to 6 donors, while hydrogen bond donor groups have 1 to 3 donors. The polar surfaces of most compounds are around 70.67 square angstroms, with polar columns ranging from 60 to 90 square angstroms. The iLOGP index for all compounds is below 1.84, indicating low hydrophobicity. Additionally, all studied compounds exhibit high solubility in physiological fluids (**Table 3**).

Pharmaceutical Properties of Studied Compounds:

Kojic acid and other compounds that have been studied demonstrate high gastrointestinal absorption but are unable to penetrate the blood-brain barrier. They also do not inhibit cytochrome P450 enzymes and are not Pgp substrates. Additionally, these compounds show minimal absorption through the skin. The Abbot Bioavailability Score (ABS) assesses compounds based on three factors and places them into four categories with probabilities ranging from 11% to 85%. The goal of ABS is to quickly identify promising molecules for further development in medicinal chemistry projects. In our study, the Bioavailability Score for all compounds examined was 55%.
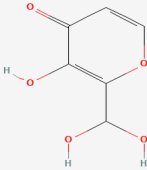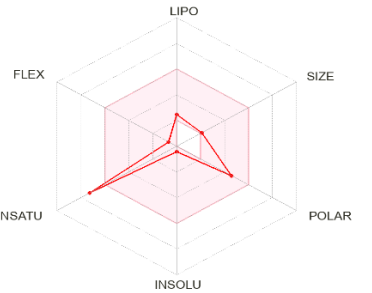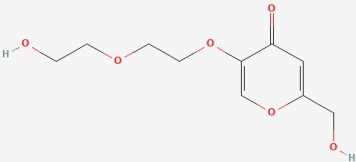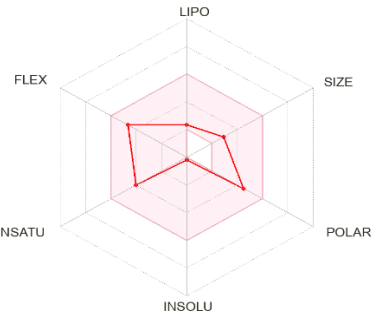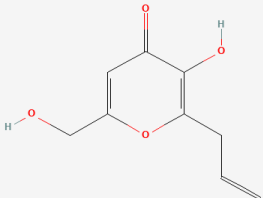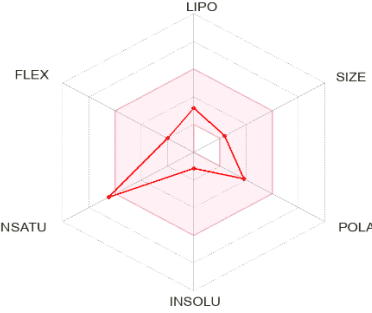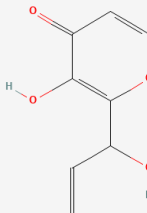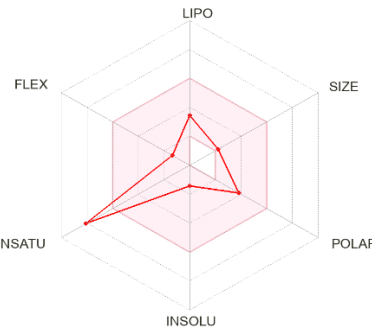
The SwissADME Synthetic Accessibility (SA) Score measures the ease or difficulty of synthesizing a molecule, with scores ranging from 1 (very easy) to 10 (very hard). A lower score indicates that the compound is more likely to be synthesized. In our study, most of the compounds analyzed had SA scores below 3, indicating that their synthesis is not challenging. (Refer to **Table 4** and **Figure 4** for more details).

DISCUSSION

The melanogenic enzymes tyrosinase (TYR), tyrosinase-related protein 1 (TYRP1), and tyrosinase-related protein 2 (TYRP2) play a crucial role in the biosynthesis of melanin, a pigment responsible for the coloration of the skin, hair, and eyes. Mutations in the genes encoding these proteins have been linked to various disorders, including loss of skin pigmentation, which can increase the risk of developing carcinoma, as well as abnormal development of the retina, leading to severe visual defects [21].
The crystal structure of the intra-melanosomal domain of TYRP1 has revealed that it contains two zinc ions bound in a binuclear site, similar to bacterial and fungal tyrosinases [22]. This finding suggests that TYRP1 may have a different activity from TYR, which is supported by experimental evidence [2, 23].

Table 1. The IUPAC name, 2D structure, and Bioavailability Radar scale of the studied compounds. This scale allows for a rapid assessment of a molecule's drug-likeness, with the ideal range for each property highlighted in the pink area.

| Name or IUPAC Name	2D- Structure of the studied compounds	Bioavailability Radar scale of the studied compounds
2-(dihydroxymethyl)-3-hydroxypyran-4-one		
5-[2-(2-hydroxyethoxy)ethoxy]-2-(hydroxymethyl)pyran-4-one		
3-hydroxy-6-(hydroxymethyl)-2-prop-2-enylpyran-4-one		
3-hydroxy-2-(1-hydroxyprop-2-enyl)pyran-4-one		

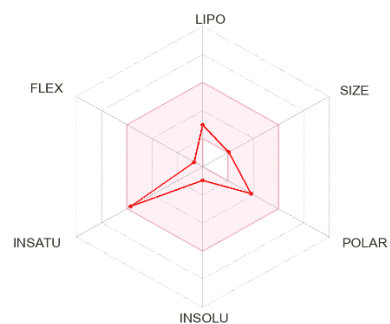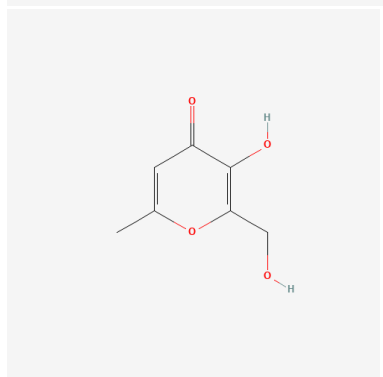5-(2-Hydroxyethoxy)-2-(hydroxymethyl)pyran-4-one
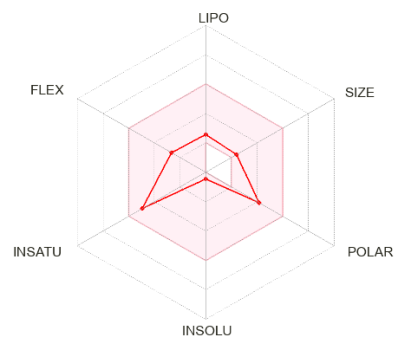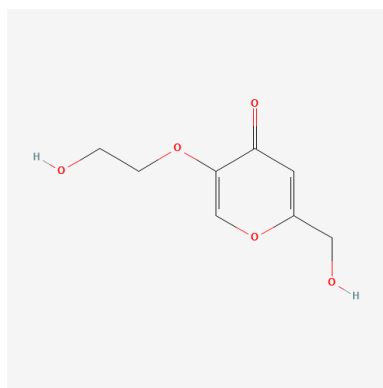
2-(hydroxymethyl)-5-(3-hydroxypropoxy)pyran-4-one
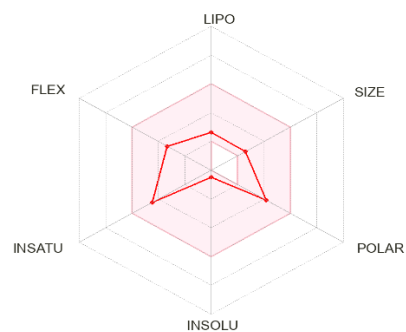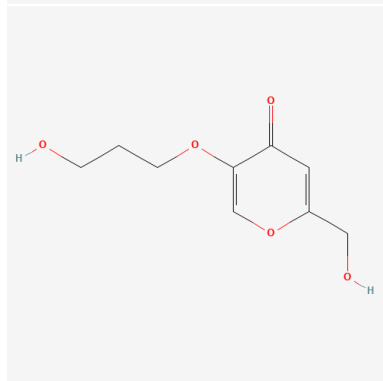
3-hydroxy-2,6-bis(hydroxymethyl)pyran-4-one
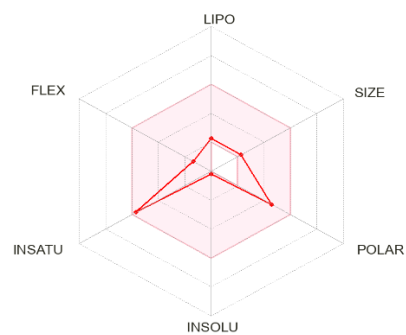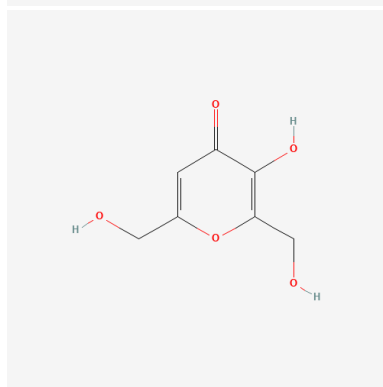
3-hydroxy-2-(hydroxymethyl)-6-methylpyran-4-one

3,5-dihydroxy-2-(hydroxymethyl)pyran-4-one

2-(hydroxymethyl)-5-methoxypyran-4-one

2-ethyl-3-hydroxy-6-(hydroxymethyl)pyran-4-one

6-(fluoromethyl)-3-hydroxy-2-(hydroxymethyl)pyran-4-one

6-ethyl-3-hydroxy-2-
(hydroxymethyl)pyran-4-one
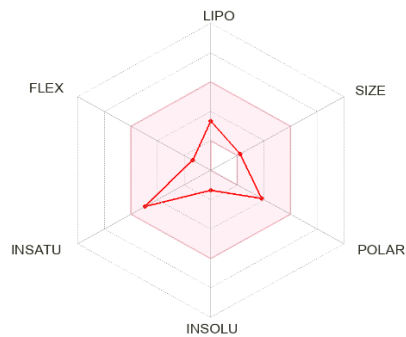
3-hydroxy-2-(hydroxymethyl)pyran-
4-one
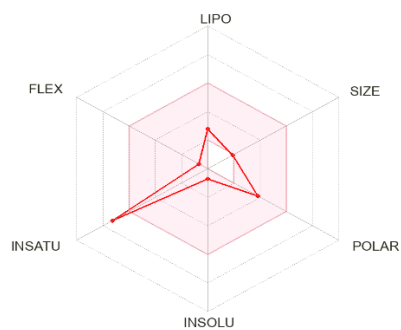
5-hydroxy-2-(hydroxymethyl)pyran-
4-one
(Kojic acid)

6-(hydroxymethyl)-4-oxopyran-3-
olate

3-hydroxy-6-(hydroxymethyl)-2-iodopyran-4-one

3-hydroxy-2-(1-hydroxyethyl)pyran-4-one
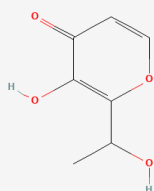
2-bromo-3-hydroxy-6-(hydroxymethyl)pyran-4-one
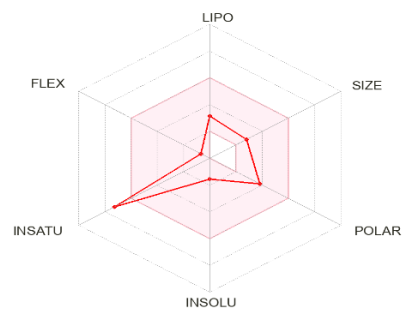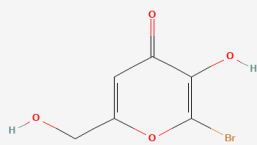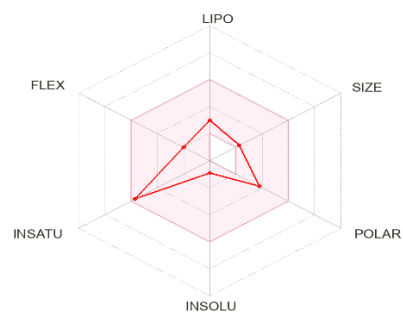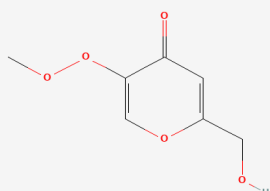
2-(hydroxymethyl)-5-methylperoxypyran-4-one

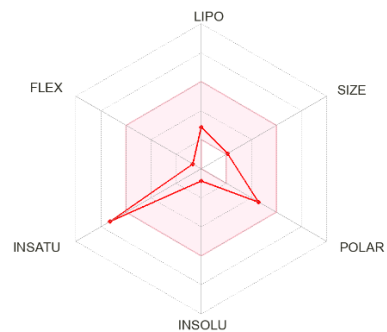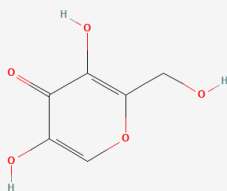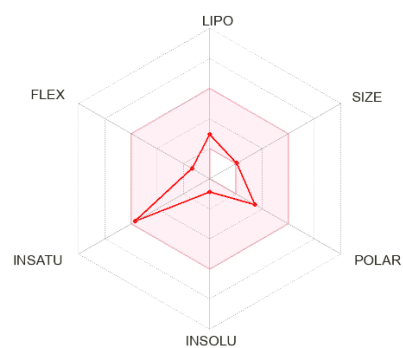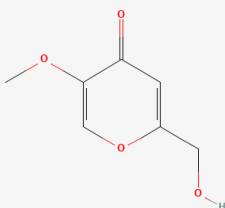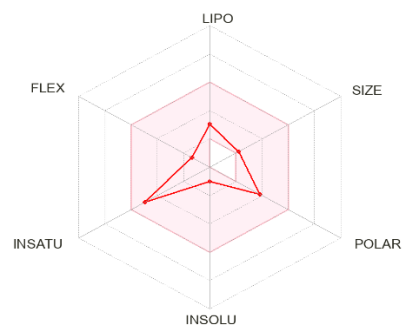2-chloro-3-hydroxy-6-(hydroxymethyl)pyran-4-one
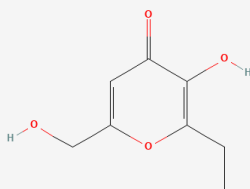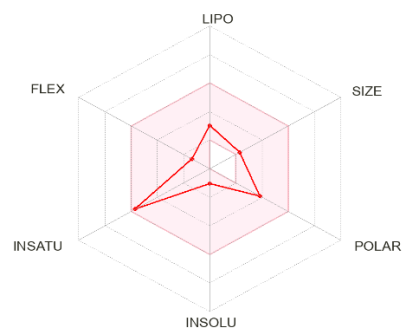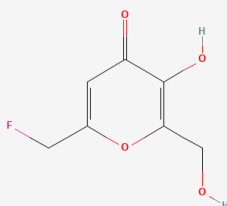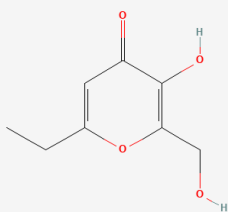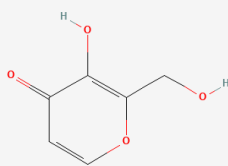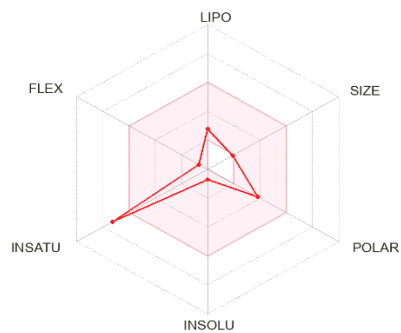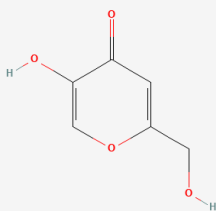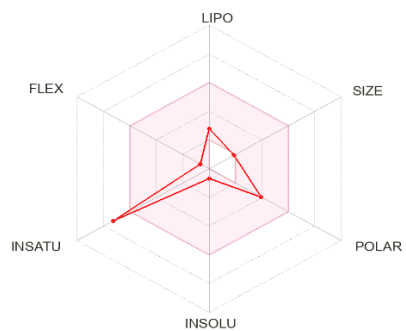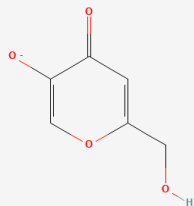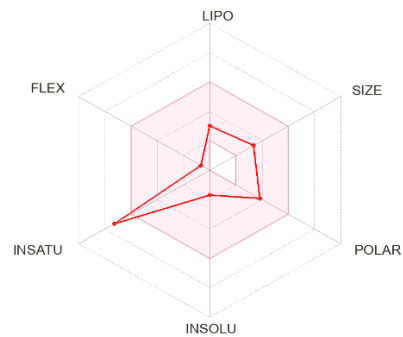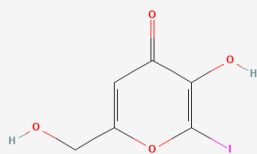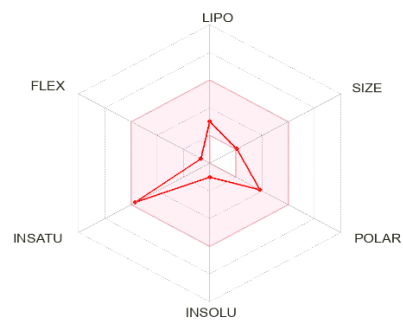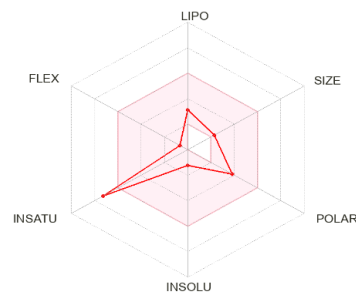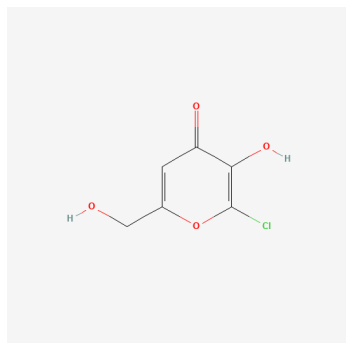

3-hydroxy-6-(hydroxymethyl)-2-methylpyran-4-one
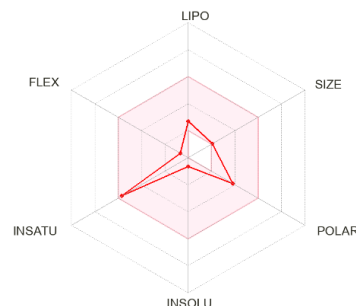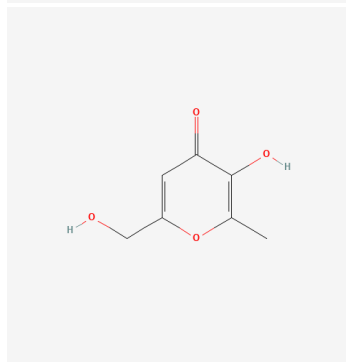
TYRP1 is a 5,6-dihydroxyindole-2-carboxylic acid oxidase that plays a crucial role in melanin biosynthesis. It catalyzes the oxidation of 5,6-dihydroxyindole-2-carboxylate into indole-5,6-quinone-2-carboxylate. The protein also has the ability to hydroxylate tyrosine and produce melanin [23], [24].

The binding of L-tyrosine and L-DOPA analogues to TYRP1 has been investigated, revealing that these compounds do not directly interact with the zinc ions. In contrast, tyrosine analogues such as tyrosol have been shown to coordinate copper ions in bacterial tyrosinases. TYRP1 does not exhibit tyrosinase redox activity [25]. Furthermore, protein structures reveal that the Cys-rich subdomain, unique to vertebrate melanogenic proteins, has an epidermal growth factor-like fold and is tightly associated with the tyrosinase subdomain [26]. These findings suggest that most albinism-related mutations of TYRP1 affect its stability or activity [26].

The human melanogenic pathway involves three enzymes: tyrosinase (TYR), tyrosinase-related protein 2 (TYRP2), and tyrosinase-related protein 1 (TYRP1). TYR is the rate-limiting enzyme that catalyzes the hydroxylation and oxidation of tyrosine. TYRP2 is a tautomerase, while TYRP1 has been suggested to catalyze the oxidation of 5,6-dihydroxyindole-2-carboxylic acid (DHICA) in mice, although this activity has been challenged in humans (2^7). All three enzymes are metal-containing glycoproteins localized in melanosomes, where melanin synthesis takes place. Mutations in the TYR or TYRP1 genes result in oculocutaneous albinism (OCA), a group of autosomal recessive disorders characterized by reduced production of melanin in skin, hair, and eyes. In addition, TYR and TYRP1 variants are significantly associated with the risk of melanoma, a malignant tumor of melanocytes that is responsible for most deaths related to skin cancer [25]-[27].

The inhibition of tyrosinase activity is an effective strategy for preventing excessive melanin synthesis. Kojic acid and β-arbutin are two well-known depigmenting agents that have been shown to inhibit tyrosinase activity. These compounds are commonly used as positive controls in assays to screen for emerging components or extracts that effectively inhibit melanin synthesis [11-13].

In our study, physicochemical and pharmaceutical properties of kojic acid and its analog compounds were investigated. The results showed that all 22 compounds studied had high gastrointestinal absorption rates, but none were predicted to be blood-brain barrier (BBB) permeant or P-glycoprotein (Pgp) substrates or inhibitors of cytochrome P450 enzymes, such as CYP1A2, CYP2C19, and CYP3A4. The log Kp values ranged from -6.9 to -8.7, indicating low levels of skin permeability. The bioavailability scores ranged from 0.55 to 0.85, indicating moderate levels of bioavailability. The synthetic accessibility scores ranged from 2.50 to 3.27, indicating varying levels of ease with which they can be synthesized.
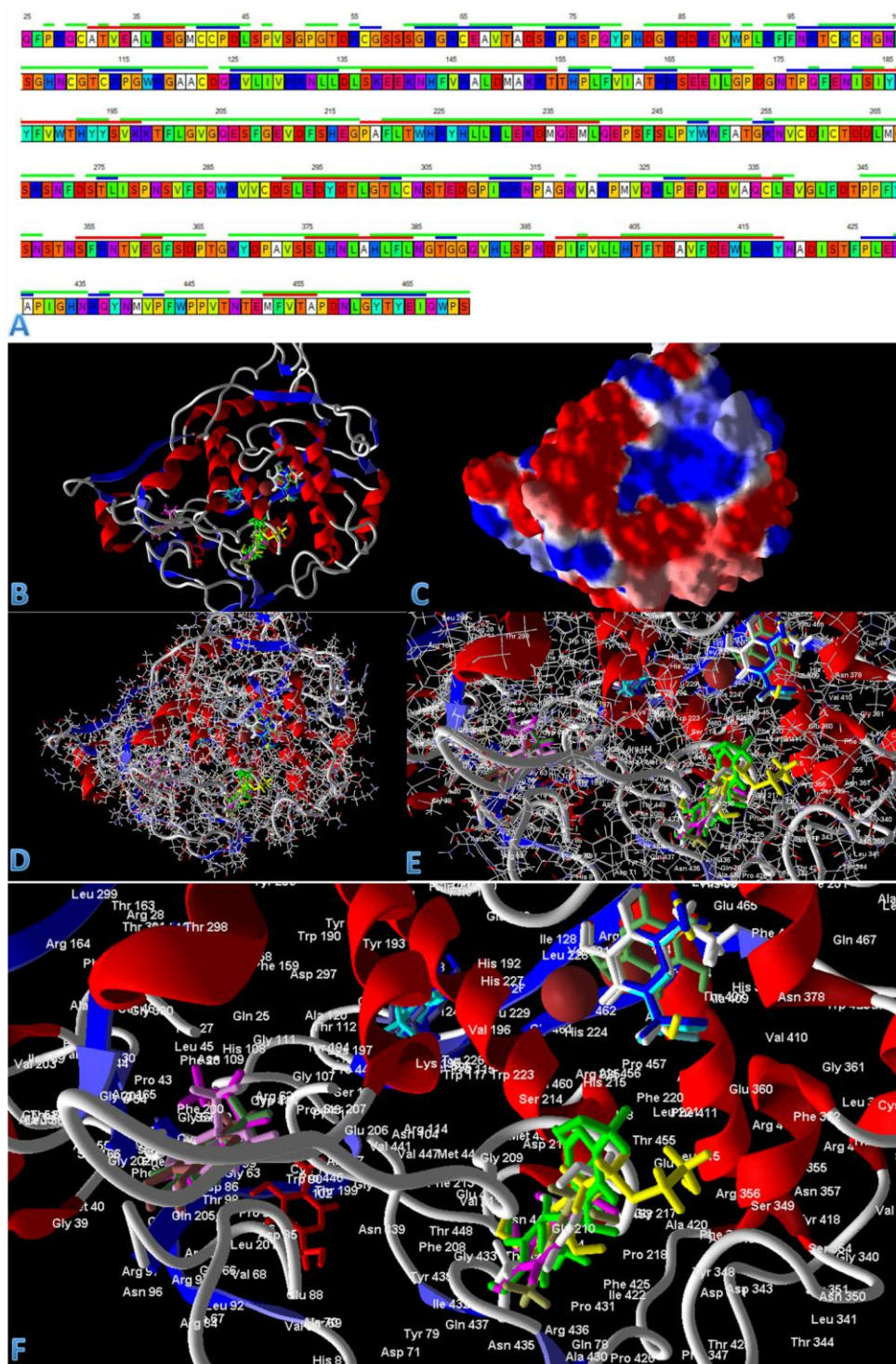
Figure 1. The amino acid sequences of tyrosinase-related protein 1 (TRP1), which includes amino acids 25-470, as well as the TRP1 model [PDB ID: 5M8T]. The docking study using this model identified cavities, highlighted with a green ribbon at the top of the sequence, indicating the amino acids that cover these areas. Additionally, blue ribbons above the sequences signify beta-sheet secondary structure, while red ribbons indicate alpha helix structure (A). The figure also includes a secondary structure model of TRP1 (B), an electrostatic surface model (C), a wireframe model of TRP1 in connection with studied inhibitors (D and E), and the binding sites of studied inhibitors with TRP1 (F).
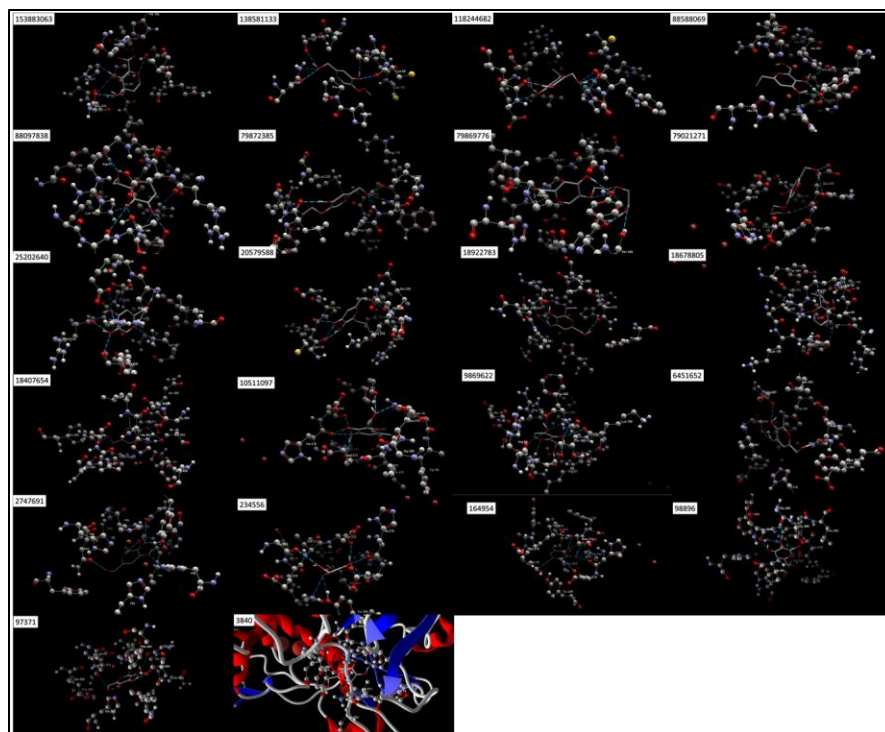
Figure 2. The binding site of the studied tyrosinase-related protein 1 (TRP1) inhibitor compounds on the enzyme model of TRP1 [PDB ID: 5M8T], with hydrogen bonds depicted by blue dotted lines. The enzyme model is illustrated as a ball and stick model. The CID number for each ligand is displayed in the upper left-hand corner of each image.
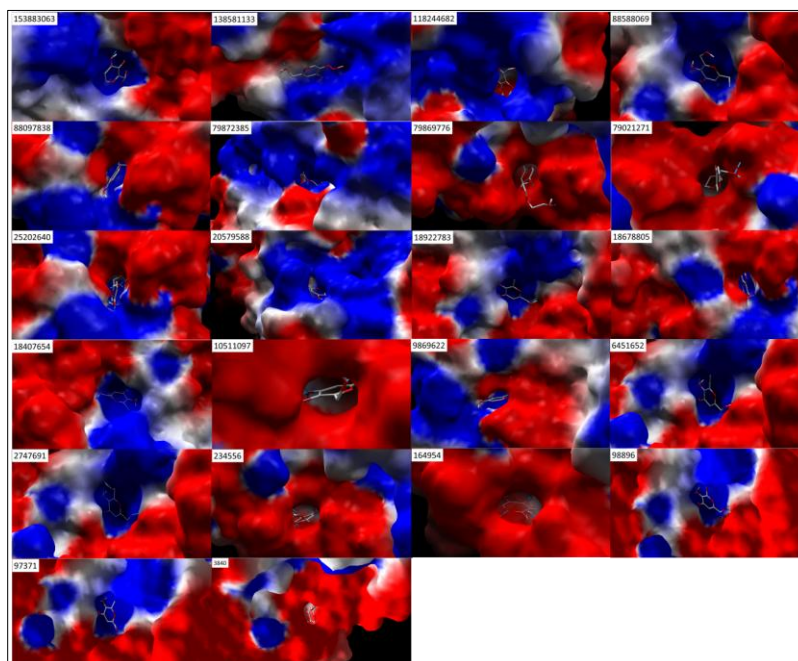
Figure 3. The binding site of the studied TRP1 inhibitor compounds on the enzyme model of TRP1 [PDB ID: 5M8T], with the enzyme model represented as electrostatic surfaces. The CID number for each ligand is displayed in the upper left-hand corner of each image.

Table 2. The molecular docking results of the studied compounds binding to the TRP1 model [PDB ID: 5M8T].

Name or IUPAC Name	CID Number	MolDock Score (kcal/mol)	Heavy Atoms	MW	Torsions	Interaction (The total interaction energy between pose and the targets molecules) (kcal/mol)	Cofactor (The interaction energy between pose and the cofactors) (kcal/mol)	Protein (The interaction energy between pose and the protein) (kcal/mol)	Internal (The internal energy of the pose) (kcal/mol)	H-Bond (kcal/mol)	LE1 (kcal/mol)
2-(dihydroxymethyl)-3-hydroxypyran-4-one	153883063	-115.357	11	156.093	1	-125.101	-36.442	-88.6593	9.7442	-4.82266	-10.487
5-[2-(2-hydroxyethoxy)ethoxy]-2-(hydroxymethyl)pyran-4-one	79869776	-109.103	16	231.222	7	-111.401	0	-111.401	2.29773	-11.8064	-6.81894
3-hydroxy-6-(hydroxymethyl)-2-prop-2-enylpyran-4-one	20579588	-100.104	13	184.189	3	-98.1904	0	-98.1904	-1.91407	-6.82732	-7.70034
3-hydroxy-2-(1-hydroxyprop-2-enyl)pyran-4-one	88097838	-99.3943	12	170.163	2	-105.776	0	-105.776	6.38173	-12.8858	-8.28286
5-(2-Hydroxyethoxy)-2-(hydroxymethyl)pyran-4-one	79872385	-97.9715	13	187.17	4	-96.7185	0	-96.7185	-1.25304	-11.5	-7.53627
2-(hydroxymethyl)-5-(3-hydroxypropoxy)pyran-4-one	79021271	-97.0127	14	201.197	5	-97.2358	0	-97.2358	0.223076	-4.92841	-6.92948
3-hydroxy-2,6-bis(hydroxymethyl)pyran-4-one	2747691	-94.1888	12	173.143	2	-89.8689	-4.02814	-85.8408	-4.31988	-8.7208	-7.84906
3-hydroxy-2-(hydroxymethyl)-6-methylpyran-4-one	10511097	-92.6252	11	157.144	1	-92.0437	0	-92.0437	-0.58144	-8.69183	-8.42047
3,5-dihydroxy-2-(hydroxymethyl)pyran-4-one	164954	-92.5495	11	159.117	1	-90.7558	0	-90.7558	-1.7937	-7.5387	-8.41359
2-(hydroxymethyl)-5-methoxypyran-4-one	234556	-89.5569	11	157.144	2	-89.8367	0	-89.8367	0.279805	-4.1335	-8.14154
2-ethyl-3-hydroxy-6-(hydroxymethyl)pyran-4-one	189922783	-89.2141	12	171.171	2	-90.708	-4.66227	-86.0457	1.49393	-4.84944	-7.4345

Compound												
6-(fluoromethyl)-3-hydroxy-2-(hydroxymethyl)pyran-4-one	88588069	-88.8072	12	175.134	2	-89.7531		-4.12802	-85.6251	0.945885	-4.07004	-7.4006
6-ethyl-3-hydroxy-2-(hydroxymethyl)pyran-4-one	118244682	-88.0736	12	171.171	2	-88.7111		0	-88.7111	0.637539	-11.5409	-7.33947
3-hydroxy-2-(hydroxymethyl)pyran-4-one	9869622	-87.8474	10	143.117	1	-89.949		0	-89.949	2.10163	-12.2319	-8.78474
5-hydroxy-2-(hydroxymethyl)pyran-4-one (Kojic acid)	3840	-87.084	10	143.117	1	-86.9741		0	-86.9741	-0.10993	-6.4754	-8.7084
6-(hydroxymethyl)-4-oxopyran-3-olate	25202640	-86.1174	10	143.117	1	-89.6989		0	-89.6989	3.58155	-7.43042	-8.61174
3-hydroxy-6-(hydroxymethyl)-2-iodopyran-4-one	6451652	-85.4242	11	269.013	1	-83.959		-4.17436	-79.7846	-1.46526	-6.26624	-7.76584
3-hydroxy-2-(1-hydroxyethyl)pyran-4-one	18678805	-85.3679	11	157.144	1	-87.8049		0	-87.8049	2.43699	-7.82583	-7.76072
2-bromo-3-hydroxy-6-(hydroxymethyl)pyran-4-one	98896	-85.1095	11	222.013	1	-84.3424		-4.14574	-80.1966	-0.76711	-6.34024	-7.73722
2-(hydroxymethyl)-5-methylperoxypyran-4-one	138581133	-84.289	12	173.143	3	-84.0785		0	-84.0785	-0.2105	-5.95936	-7.02408
2-chloro-3-hydroxy-6-(hydroxymethyl)pyran-4-one	18407654	-83.378	11	177.562	1	-83.2083		-4.25252	-78.9558	-0.16966	-4.86975	-7.57981
3-hydroxy-6-(hydroxymethyl)-2-methylpyran-4-one	97371	-83.1516	11	157.144	1	-82.7414		-4.23805	-78.5033	-0.41024	-4.02145	-7.55924

Table3. Physicochemical Properties of Studied Compounds

Molecule	Formula	Heavy atoms	Aromatic heavy atoms	Fraction Csp3	Rotatable bonds	H-bond acceptors	H-bond donors	MR	TPSA	iLOGP	XLOGP3	ESOL Solubility (mg/ml)	ESOL Class
153883063	C6H6O5	11	6	0.17	1	5	3	34.29	90.90	0.90	-1.16	59.1	Very soluble
79869776	C10H14O6	16	6	0.50	7	6	2	54.27	89.13	1.84	-1.40	145	Very soluble
20579588	C9H10O4	13	6	0.22	3	4	2	47.23	70.67	1.62	0.09	12.3	Very soluble
88097838	C8H8O4	12	6	0.12	2	4	2	42.27	70.67	1.50	0.50	61.7	Very soluble
79872385	C8H10O5	13	6	0.38	4	5	2	43.57	79.90	1.54	-1.00	67.1	Very soluble
79021271	C9H12O5	14	6	0.44	5	5	2	48.37	79.90	1.59	-0.90	63.1	Very soluble
2747691	C7H8O5	12	6	0.29	2	5	3	39.26	90.90	1.11	-1.51	110	Very soluble
10511097	C7H8O4	11	6	0.29	1	4	2	38.09	70.67	1.34	-0.26	16.3	Very soluble
164954	C6H6O5	11	6	0.17	1	5	3	35.15	90.90	1.01	-0.49	22.4	Very soluble

CID	Formula													Solubility
18407654	C6H5ClO4	11	6	0.17	1	4	2	38.14	70.67	1.22	-0.06	10.3		Very soluble
138581133	C7H8O5	12	6	0.29	3	5	1	38.68	68.90	1.62	-0.27	21.2	Very soluble	
98896	C6H5BrO4	11	6	0.17	1	4	2	40.83	70.67	1.26	0.01	61.7	Very soluble	
18678805	C7H8O4	11	6	0.29	1	4	2	37.94	70.67	1.44	-0.21	15.1	Very soluble	
25202640	C6H5O4-	10	6	0.17	1	4	1	31.24	73.50	1.23	-0.64	28.8	Very soluble	
6451652	C6H5IO4	11	6	0.17	1	4	2	45.85	70.67	1.40	-0.24	5.5	Very soluble	
9869622	C6H6O4	10	6	0.17	1	4	2	33.13	70.67	1.08	-0.61	27.4	Very soluble	
118244682	C8H10O4	12	6	0.38	2	4	2	42.90	70.67	1.68	0.37	7.32	Very soluble	
88588069	C7H7FO4	12	6	0.29	2	5	2	38.15	70.67	1.33	-0.19	16.1	Very soluble	
18922783	C8H10O4	12	6	0.38	2	4	2	42.90	70.67	1.74	-0.18	16.3	Very soluble	
234556	C7H8O4	11	6	0.29	2	4	1	37.60	59.67	1.82	-0.31	20.4	Very soluble	

	97371	3840
	C7H8O4	C6H6O4
	11	10
	6	6
	0.29	0.17
	1	1
	4	4
	2	2
	38.09	33.13
	70.67	70.67
	1.48	1.12
	-0.81	-0.64
	36.2	28.6
	Very soluble	Very soluble

Table 4. Pharmaceutical Properties of Studied Compounds

Moleculе	GI absorption	BBB permeant	Pgp substrate	CYP1A2 inhibitor	CYP2C19 inhibitor	CYP2C9 inhibitor	CYP2D6 inhibitor	CYP3A4 inhibitor	log Kp (cm/s)	Bioavailability Score	Synthetic Accessibility
153883063	High	No	No	No	No	No	No	No	-8.09	0.55	2.58
79869776	High	No	No	No	No	No	No	No	-8.70	0.55	3.10
20579588	High	No	No	No	No	No	No	No	-7.35	0.55	2.98
88097838	High	No	No	No	No	No	No	No	-6.97	0.55	3.27
79872385	High	No	No	No	No	No	No	No	-8.15	0.55	2.80
79021271	High	No	No	No	No	No	No	No	-8.16	0.55	2.81
2747691	High	No	No	No	No	No	No	No	-8.42	0.55	2.68

ID											
10511097	High	No	No	No	No	No	No	No	-7.44	0.55	2.64
164954	High	No	No	No	No	No	No	No	-7.61	0.55	2.58
234556	High	No	No	No	No	No	No	No	-7.47	0.55	2.59
18922783	High	No	No	No	No	No	No	No	-7.47	0.55	2.74
88588069	High	No	No	No	No	No	No	No	-7.50	0.55	2.57
118244682	High	No	No	No	No	No	No	No	-7.08	0.55	2.77
9869622	High	No	No	No	No	No	No	No	-7.60	0.55	2.51
6451652	High	No	No	No	No	No	No	No	-8.11	0.55	2.95
25202640	High	No	No	No	No	No	No	No	-7.62	0.85	2.50
18678805	High	No	No	No	No	No	No	No	-7.40	0.55	3.01
98896	High	No	No	No	No	No	No	No	-7.64	0.55	2.65

	138581133	18407654	97371	3840
	High	High	High	High
	No	No	No	No
	No	No	No	No
	No	No	No	No
	No	No	No	No
	No	No	No	No
	No	No	No	No
	No	No	No	No
	-7.54	-7.42	-7.83	-7.62
	0.55	0.55	0.55	0.55
	3.13	2.61	2.63	2.53

In our study, the binding site of kojic acid and its analog compounds with CID numbers 79869776, 79021271, 10511097, 234556, 164954, and 3840 contains amino acids Gln78, Gly209, Glu210, Val211, Asp212, Phe213, His215, Glu216, Tyr348, Ser349, Pro431, and Ile432 from the sequence of tyrosinase-related protein 1. Similarly, the compounds with CID numbers 97371, 98896, 2747691, 6451652, 18407654, 18922783, and 88588069 bind to a binding site containing amino acids His192, His215, His377, Asn378, His381, Leu382, Gly389, Gln390, Val391, Ser394, and Phe400 from the tyrosinase sequence-related protein 1.

The crystal structure of TYRP1 has been reported, revealing a binuclear metal-binding site similar to the classical type-3 binuclear copper-binding site of hemocyanins and tyrosinases. However, the identity of the bound metal ions was previously unclear. X-ray fluorescence analysis showed that TYRP1 crystals contained zinc, while TYR crystals contained copper [2, 25-29].

The active site of TYRP1 consists of two zinc ions in a nearly planar trigonal geometry, slightly out of the plane defined by the Nε2 atoms of their ligands. The distance between ZnA and ZnB ions is 3.5±0.1 Å. A bridging water molecule or hydroxide ion can be modeled with a distance of 2.1±0.1 Å to the two zinc ions (2, 25-29). This discovery has significant implications for understanding the role of TYRP1 in melanogenesis. The Cys-rich subdomain of TYRP1 has an epidermal growth factor (EGF)-like fold, resembling the structure of human epidermal growth factor [29]. This fold consists of two pairs of short antiparallel beta-strands (beta1/beta2 and beta4/beta5) with long loops extending from them. The subdomain is stabilized by disulfide bonds following the [C1-C3, C2-C4, C5-C6] signature pattern of EGF-like structures [2, 25, 26, 29].

The Cys-rich subdomain interacts with the tyrosinase-like subdomain through its N-terminus and the long 67-97 loop extending from the core [30]. Despite being located far from the active site, the subdomain is unlikely to directly affect TYRP1 activity. While the Cys-rich subdomain has been proposed to play a role in oligomerization, no evidence was found to support this, as both purified intramelanosomal domains of TYRP1 and TYR elute as monomers on size-exclusion chromatography, and co-elution of TYRP1 and TYR did not result in a heterodimer [29-31].

TYRP1 lacks DHICA activity, and the intramelanosomal domain of TYRP1 does not exhibit DHICA activity, tyrosine hydroxylase activity, or l-DOPA oxidase activity (28). The differences in activity are partly attributed to the nature of the metal ions in the active site. Swapping the Zn2+/Cu2+ cofactors of TYRP1/TYR for Cu2+/Zn2+ led to the acquisition of TYR-level DHICA oxidase activity by TYRP1, without significant l-DOPA oxidase and tyrosine hydroxylase activities (2, 28, 29).

The binding of phenylthiourea (PTU) to tyrosinase-related protein 1 (TYRP1) is unique compared to other tyrosinase inhibitors. PTU does not coordinate the active site zinc ions, and instead, its aromatic ring faces outward from the active site due to the absence of polar oxygen substituents. The binding of PTU is facilitated by hydrophobic interactions with the side chains of Phe362, Leu382, and Val391, which obstruct substrate access to the active site [2, 29-31].
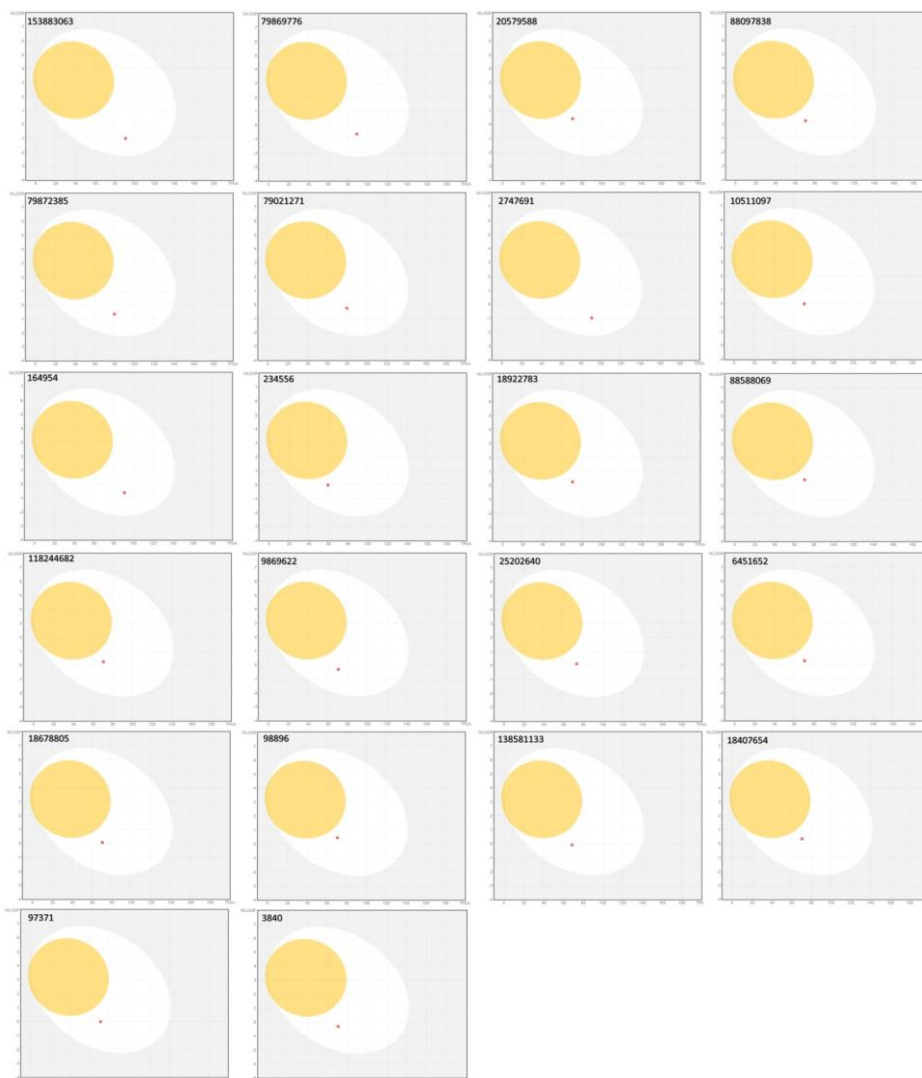
Figure 4. The egg plot, visually representing a compound's ability to interact with the blood-brain barrier, digestive system, and substrate for P-glycoproteins. Yellow indicates passive crossing of the blood-brain barrier, white indicates passive absorption by the digestive system, blue dots represent entry into the central nervous system through P-glycoproteins, and red dots represent exit from the central nervous system through P-glycoproteins.

The PTU aromatic ring is oriented outward from the binuclear zinc site, stabilized by hydrophobic interactions with the side chains of Phe362, Leu382, and Val391. The thiourea amino group forms hydrogen bonds with the backbone oxygen of Gly389 and a water molecule (W4), while the amide nitrogen and thiourea sulfur form hydrogen bonds with water molecules W3 and W2, respectively [25-29].

Interestingly, PTU does not interact with the binuclear metal site, but instead hinders substrate access to the active site. This distinctive binding mode is supported by comparing the PTU-inhibited TYRP1-3M structure with TYRP1-3M structures bound to kojic acid,

mimosine, and tropolone. In the PTU-inhibited structure, TYRP1-3M (which is a mutant with three non-conserved active site residues replaced by Y362F/R374S/T391V), the aromatic ring of PTU points outward from the active site, unlike other inhibitors whose ring system faces the binuclear metal-binding site [25, 29, 32].

The amide nitrogen of PTU aligns perfectly with the ring C5 carbon atom of kojic acid, the ring nitrogen atom of mimosine, and the $C\alpha 5$ carbon atom of tropolone. The space occupied by water molecules W2 and W3 in the PTU-bound structure is taken by the ring oxygen atoms of kojic acid, mimosine, and tropolone, forming hydrogen bonds with the bridging water

molecule W1 between the two metal ions in the active site [29]. The PTU sulfur atom coincides with a ring carbon atom of the inhibitors (e.g., the Cε atom of the mimosine ring) [25-29].

Fifteen OCA-related mutations in the TYRP1 gene have been identified, including 8 point mutations (C30R, R93C, H215Y, T253M, C290Y, R356Q, M452V, and P513R) (30). Most of these residues contribute to enzyme stability. The C30–C41 disulfide bond links helix α1 to the core of the Cys-rich subdomain, the C290–C303 disulfide bond stabilizes the 290–303 loop, and R356 is involved in a buried hydrogen-bonding network. H215 serves as a ZnA ligand, and substitution by Tyr could weaken the enzyme's zinc-binding affinity and activity. In our study, H215 played an important role in binding most of the compounds studied to the enzyme[2, 25-29, 32].

CONCLUSION

This study focused on inhibiting hyperpigmentation and melanin biosynthesis by molecular docking kojic acid and its analogues as inhibitors of the TYRP1 enzyme. Physicochemical properties and inhibitor binding sites were analyzed. Our study delved into the enzyme's structure, critical amino acids in the active site, and the binding sites of the inhibitors under investigation. We also investigated mutations linked to TYRP1 inactivation, providing insights into its function and inhibition. The results of our molecular docking study revealed that kojic acid and its structural analogues exhibit a strong affinity for the active site of TYRP1. These findings offer insight into the molecular mechanisms of TYRP1 inhibition and could assist in developing more potent and selective inhibitors.

Conflict of interest
The author declares that there isn't any conflict of interest regarding the publication of this paper.

REFERENCES

1. Kanlayavattanakul M, Lourith N. Plants and natural products for the treatment of skin hyperpigmentation–a review. *Planta medica*. **2018** *84*(14):988-1006.

2. Lai X, Wichers HJ, Soler-Lopez M, Dijkstra BW. Structure of human tyrosinase related protein 1 reveals a binuclear zinc active site important for melanogenesis. *Angewandte Chemie International Edition*. **2017** ;56(33):9812-5.

3. Gopinath H, Karthikeyan K. Turmeric: A condiment, cosmetic and cure. *Indian journal of dermatology, venereology and leprology*. **2018**, 84:16.

4. Humbert P, Louvrier L, Saas P, Viennet C. Vitamin c, aged skin, skin health. InVitamin C-an Update on *Current Uses and Functions* **2018**, 5. IntechOpen.

5. Desai SR. Hyperpigmentation therapy: a review. *The Journal of clinical and aesthetic dermatology*. **2014**, 7(8):13.

6. Benmaman O, Sanchez JL. Treatment and camouflaging of pigmentary disorders. *Clinics in Dermatology.* **1988**, 6(3):50-61.

7. Jackson IJ. Homologous pigmentation mutations in human, mouse and other model organisms. *Human molecular genetics*. **1997** ;6(10):1613-24.

8. Böer-Auer A. New aspects in the histopathology of infectious skin diseases. *Wiener klinisches Magazin.* **2021**; 24:20-33.

9. Getting SJ. Targeting melanocortin receptors as potential novel therapeutics. *Pharmacology & therapeutics.* **2006** ;111(1):1-5.

10. Vance KW, Goding CR. The transcription network regulating melanocyte development and melanoma. *Pigment cell research*. **2004**, 17(4):318-25.

11. Lee YS, Park JH, Kim MH, Seo SH, Kim HJ. Synthesis of tyrosinase inhibitory kojic acid derivative. *Archiv der Pharmazie: An International Journal Pharmaceutical and Medicinal Chemistry*. **2006**, 339(3):111-4.

12. Hong JH, Chen HJ, Xiang SJ, Cao SW, An BC, Ruan SF, Zhang B, Weng LD, Zhu HX, Liu Q. Capsaicin reverses the inhibitory effect of licochalcone A/β-Arbutin on tyrosinase expression in b16 mouse melanoma cells. *Pharmacognosy magazine*. **2018**,14(53):110.

13. Boo YC. Arbutin as a skin depigmenting agent with antimelanogenic and antioxidant properties. *Antioxidants*. **2021**, 10(7):1129.

14. Kim S, Thiessen PA, Bolton EE, Chen J, Fu G, Gindulyte A, Han L, He J, He S, Shoemaker BA, Wang J. PubChem substance and compound databases. *Nucleic acids research*. **2016**; 44(D1):D1202-13.

15. Bitencourt-Ferreira G, de Azevedo WF. Molegro virtual docker for docking. *Docking screens for drug discovery.* **2019**,149-67.

16. Daina A, Michielin O, Zoete V. SwissADME: a free web tool to evaluate pharmacokinetics, drug-likeness and medicinal chemistry friendliness of

small molecules. Scientific reports. **2017**; 7(1):42717.

17. Daina A, Michielin O, Zoete V. iLOGP: a simple, robust, and efficient description of n-octanol/water partition coefficient for drug design using the GB/SA approach. *Journal of chemical information and modeling.* **2014**; 54(12):3284-301.

18. Daina A, Zoete V. A boiled-egg to predict gastrointestinal absorption and brain penetration of small molecules. *ChemMedChem.* **2016**; 11(11):1117-21.

19. Yousefi R. The Potential Application of Roselle Extracts (Hibiscus sabdariffa L.) in Managing Diabetes Mellitus. *Journal of Advanced Pharmacy Research.* **2024**, 8(2):38-48.

20. Yousefi R. Binding of curcumin near the GBT440 binding site at the alpha cleft in the sickle cell hemoglobin model [Pdb ID: 1NEJ]. *Journal of advanced Biomedical and Pharmaceutical Sciences.* **2024**, 7(2):70-4.

21. Xu Y, Zhang XH, Pang YZ. Association of tyrosinase (TYR) and tyrosinase-related protein 1 (TYRP1) with melanic plumage color in Korean quails (Coturnix coturnix). *Asian-Australasian journal of animal sciences.* **2013**, 26(11):1518.

22. Lai X, Wichers HJ, Soler-Lopez M, Dijkstra BW. Structure and function of human tyrosinase and tyrosinase-related proteins. *Chemistry–A European Journal.* **2018**; 24(1):47-55.

23. Dolinska MB, Wingfield PT, Young KL, Sergeev YV. The TYRP1-mediated protection of human tyrosinase activity does not involve stable interactions of tyrosinase domains. Pigment cell & melanoma research. **2019**; 32(6):753-65.

24. Dolinska MB, Young KL, Kassouf C, Dimitriadis EK, Wingfield PT, Sergeev YV. Protein stability and functional characterization of intra-melanosomal domain of human recombinant

tyrosinase-related protein 1. *International Journal of Molecular Sciences.* **2020** ;21(1):331.

25. Lai X, Wichers HJ, Soler-López M, Dijkstra BW. Phenylthiourea binding to human tyrosinase-related protein 1. *International journal of molecular sciences.* **2020** ;21(3):915.

26. Olivares C, Solano F. New insights into the active site structure and catalytic mechanism of tyrosinase and its related proteins. Pigment cell & melanoma research. **2009** ;22(6):750-60.

27. Dolinska MB, Anderson DE, Sergeev YV. In vitro characterization of the i ntramelanosomal domain of human recombinant TYRP1 and its oculocutaneous albinism type 3-related mutant variants. Protein Science. **2023** ;32(1):e4518.

28. Patel MH, Dolinska MB, Sergeev YV. Tyrp1 mutant variants associated with OCA3: computational characterization of protein stability and ligand binding. International Journal of Molecular Sciences. **2021** ;22(19):10203.

29. Ogiso H, Ishitani R, Nureki O, Fukai S, Yamanaka M, Kim JH, Saito K, Sakamoto A, Inoue M, Shirouzu M, Yokoyama S. Crystal structure of the complex of human epidermal growth factor and receptor extracellular domains. *Cell.* **2002**; 110(6):775-87.

30. Kamaraj B, Purohit R. In silico screening and molecular dynamics simulation of disease-associated nsSNP in TYRP1 gene and its structural consequences in OCA3. *BioMed research international.* **2013**; 2013(1):697051.

31. Kobayashi T, Imokawa G, Bennett DC, Hearing VJ. Tyrosinase stabilization by Tyrp1 (the brown locus protein). *Journal of Biological Chemistry.* **1998**; 273(48):31801-5.

32. Lai X. Structure and activity studies of tyrosinases and related proteins. University of Groningen, **2017**. p121.